JOURNAL OF AEROSOL MEDICINE AND PULMONARY DRUG DELIVERY
Volume 32, Number 4, 2019

Pp. 224–241
DOI: 10.1089/jamp.2018.1488

# Development of a High-Flow Nasal Cannula and Pharmaceutical Aerosol Combination Device

Benjamin M. Spence, BS,[1] Worth Longest, PhD,[1,2,*] Xiangyin Wei, PhD,[2] Sneha Dhapare, PhD,[2] and Michael Hindle, PhD[2,*]

## Abstract

***Background:*** Aerosol drug delivery to the lungs is known to be very inefficient during all forms of noninvasive ventilation, especially when the aerosol is administered simultaneously with high-flow nasal cannula (HFNC) therapy. The objective of this study was to develop a new combination device based on vibrating mesh nebulizers that can provide continuously heated and humidified HFNC therapy as well as on-demand pharmaceutical aerosols with high efficiency.

***Methods:*** The combination device implemented separate mesh nebulizers for generating humidity (humidity nebulizer) and delivering the medical aerosol (drug nebulizer). Nebulizers were actuated in an alternating manner with the drug nebulizer delivering the medication during a portion of an adult inhalation cycle. Aerosol entered a small-volume mixing region where it was combined with ventilation gas flow and then entered a heating channel to produce small particles that are desirable for nose-to-lung administration and potentially excipient enhanced growth delivery. Three assessment methods (analytical calculations, computational fluid dynamics [CFD] simulations, and *in vitro* experiments in three-dimensional [3D] printed devices) were used to improve the mixer-heater design to minimize depositional drug losses, maintain a small device volume, ensure sufficient droplet evaporation, and control the outlet thermodynamic conditions.

***Results:*** For an initial configuration (Design 1), good agreement in performance metrics was found using the three assessment methods. Based on insights gained from the CFD simulations of Design 1, two new designs were developed and produced with 3D printing. Experimental analysis indicated that the new designs both achieved <5% depositional loss in the mixer-heater even with cyclic operation and sufficiently dried the aerosol from an initial size of 5.3 $\mu$m to an outlet size of $\sim$1.0 $\mu$m. A combination of the applied methods indicated that the desired thermodynamic conditions of HFNC therapy were also met.

***Conclusions:*** Multiple methodological approaches were used concurrently to develop a new combination device for administering HFNC therapy and simultaneous on-demand pharmaceutical aerosols to the lungs with high efficiency. The use of a small-volume mixer-heater (<100 mL), synchronization of the drug nebulizer with inhalation, and small outlet particle size should enable high efficiency lung delivery of the aerosol.

**Keywords:** high efficiency aerosol delivery, high-flow nasal cannula, high-flow therapy, noninvasive ventilation, pharmaceutical aerosols, respiratory drug delivery

## Introduction

High-flow nasal cannula (HFNC) therapy is an increasing popular form of noninvasive ventilation (NIV) for both adult and pediatric patients with respiratory failure or insufficiency.[1–4] Subjects receiving HFNC therapy often have underlying lung conditions that may benefit from treatment with inhaled pharmaceutical aerosols.[5,6] As with other forms of NIV, a convenient approach is to add the inhaled medication directly to the inspired gas stream.[6,7] However, lung delivery efficiency of pharmaceutical aerosols is low during all forms of

Departments of [1]Mechanical and Nuclear Engineering and [2]Pharmaceutics, Virginia Commonwealth University, Richmond, Virginia.
*Member of ISAM.

NIV,[5,8] and is reported to be especially low during HFNC therapy.[6,9,10] For example, Perry et al.[9] reported that ex-cannula aerosol dose was <0.4% of the nominal dose at typical adult HFNC flow rates of 20 L/min (LPM) and above. Positioning a mesh nebulizer upstream of the HFNC humidity unit, Reminiac et al.[11] achieved 2%–10% of nebulized dose downstream of an *in vitro* nasal model. It is expected that these low lung delivery efficiencies are due to HFNC systems that were not originally designed for the administration of pharmaceutical aerosols.

Our group has proposed a mixer-heater system for the production of submicrometer pharmaceutical aerosols that can be used during HFNC administration.[12] This unit contained a large mixing region (aerosol reservoir) that was intended to allow for continuous nebulization with a mesh nebulizer, which avoids the need to synchronize aerosol generation with inspiration. Based on the work of Longest et al.,[13] a thin channel heating section was developed to dry the initial droplets with diameters in the range of 5 $\mu$m to submicrometer size and simultaneously heat the airstream. The study of Golshahi et al.[14] considered the reservoir mixer-heater system under steady-state HFNC conditions and found lung delivery efficiencies as high as 80% of the nebulized dose through the device, streamlined nasal cannula and a nose-mouth-throat (NMT) model.

The subsequent studies of Golshahi et al.[15,16] considered cyclic patient inspiration and maximized lung dose by passing airflow through the system only during inspiration. With deep cyclic inspiration (tidal volume $V_T = 0.93$ L) and flows consistent with HFNC, lung delivery efficiency near 70%–80% of nebulized dose could be achieved. However, efficiently emptying the large aerosol reservoir required deep inspiration.

From our previous work, this reservoir-based mixer-heater provides an efficient method to deliver pharmaceutical aerosols during NIV and HFNC.[14–17] While successful, the development process has also identified areas of potential improvement. As noted above, holding the aerosol during exhalation with minimal depositional loss requires a sufficiently sized reservoir, which then requires deep inspiration to empty the aerosol on the next inhalation. It was determined that timing the airflow was not easier than timing the firing of the nebulizer. Furthermore, true HFNC therapy support requires continuous delivery of humidified gas, even during exhalation.[18] To provide continuously humidified airflow with high efficiency aerosol delivery, a divided cannula was devised with separate inlets for the aerosol stream during inhalation and continuous HFNC gas support,[14] respectively. The addition of the reservoir mixer-heater to the HFNC system creates a setup that may be more complex than is necessary.

Current HFNC gas delivery systems are clearly inefficient at delivering inhaled pharmaceutical aerosols, with lung delivery efficiencies in the range of <0.4% to $\sim$10% of the nebulized dose.[6,9–11] The intent of these systems is to provide gas support at airflow rates of $\sim$10 LPM and above in a continuous manner that is warmed and humidified.[2] Using either a liquid chamber passover or porous filter-type approach, current humidification systems achieve relative humidity (RH) values of $\sim$100% and nasal inhalation temperatures near 37°C.[1,2,19] These devices have been shown to be clinically effective for respiratory gas support in a number of situations.[1,2,4] However, the need for the airstream to be fully saturated with water vapor (100% RH) and at 37°C for nasal inhalation has not been established. In fact, the inhalation of pure water vapor at 100% RH leading to low osmolarity in airway surface liquid (ASL) is expected to be irritating to the lungs.[20–22] DiBlasi[23] notes the concerning collection of liquid in these highly humidified nasal cannula interfaces leading to condensation rain-out and sputtering of liquid onto the face and potentially into the lungs of pediatric patients. Furthermore, the nasal surface temperature in the nasal valve and anterior turbinate region is reported to be in the range of 28°C–32°C (instantaneous range during a breath cycle),[24] such that achieving 37°C airflow temperature at the cannula outlet may not be necessary and may be uncomfortable for some subjects.

It is observed that a new system is needed that can provide HFNC therapy together with on-demand pharmaceutical aerosols at a high lung delivery efficiency. By developing a combination HFNC and pharmaceutical aerosol device, it is expected that high efficiency lung delivery of the pharmaceutical aerosol can be achieved. Moreover, it is proposed that humidity can be provided by the evaporation of isotonic saline droplets, which should help preserve the ionic balance of the lungs. The new mixer-heater system will therefore employ separate humidity (isotonic saline) and drug mesh nebulizers to provide continuously humidified airflow, while pharmaceutical aerosols are delivered only during a portion of inhalation. This approach avoids the need for temperature cycling in the heating section. Furthermore, a device providing humidity from isotonic saline droplets is currently not available and has the potential to be less irritating to the lungs compared with 100% pure water vapor.[25]

To ensure high efficiency lung delivery of the pharmaceutical aerosol, the excipient enhanced growth (EEG) approach will be implemented.[26,27] In one form, EEG approach consists of drying nebulized pharmaceutical droplets to submicrometer size, to enable high efficiency lung delivery. Once the pharmaceutical aerosol is within the airways, water uptake by the included hygroscopic excipient causes droplet size increase and enables deposition by sedimentation and impaction.[28–30] The proposed device can be used to administer bronchodilators as a standard therapy.[5] In addition, the use of the nasal interface and nebulizer design enables the continuous delivery of high-dose medications like inhaled antibiotics, mucolytics, and surfactants.[31]

The objective of this study is to develop a new device based on vibrating mesh nebulizers that can provide continuously heated and humidified high-flow nasal cannula therapy as well as on-demand pharmaceutical aerosols delivered with high efficiency using the nose-to-lung route. To develop this device, a concurrent analytical, *in vitro*, and computational fluid dynamics (CFD) approach[32,33] will be used along with three-dimensional (3D) printing of rapid prototyped physical models. Based on past experience and analytical analysis, an initial mixer-heater is first proposed, which uses a small-volume design and synchronized actuation of the nebulizers instead of actuation of the airflow. This initial design is assessed with analytical calculations, CFD, and *in vitro* analysis. Comparisons of these three methods leads to a validated CFD model that is used to better understand device performance. The validated CFD

model and *in vitro* experiments are then used to develop new designs to achieve low aerosol loss within the device, as well as targeted outlet temperature and RH conditions. Using this concurrent analytical, *in vitro*, and CFD approach, the goal of this study is to develop a combination device that achieves a high transmission efficiency of the nebulized aerosol (≥90%) when operated cyclically, produces a small particle aerosol (with a mean particle diameter of $\sim 1\,\mu$m), and can administer the inhaled medication simultaneously with HFNC therapy.

## Materials and Methods

### *Mixer-heater design*

In this study, a new small-volume mixer-heater design is proposed and evaluated, which takes advantage of mesh nebulizer actuation synchronized with the breathing cycle. A primary characteristic of this design is a minimized size of the mixing region, which will improve emptying of the aerosol from the device. This improved emptying will reduce spread of the aerosol bolus over time compared with the larger mixing region that was included in the previous mixer-heater design.[12] Improved emptying should also minimize the time delay between when the aerosol is generated and when it reaches the patient, thereby enhancing the lung delivery benefits of synchronization.

For adults, passive inhalation durations are typically 1.5 seconds or greater.[34] As a target, the mixer-heater should empty within 20% of this inhalation duration, providing an emptying time of $\sim$0.3 seconds. To achieve this emptying time at an HFNC flow rate of 20 LPM (or 333.3 $cm^3$/s), the system volume, including connective outlet tubing, should be $\sim$100 mL or less. Similarly, at 30 LPM (or 500 $cm^3$/s), an emptying time of 0.3 second can be achieved with a system volume of $\sim$150 mL or less. While reducing the system volume appears beneficial from an emptying standpoint, it is noted that the aerosol leaving the mesh nebulizer has observable momentum due to two-way momentum coupling. Therefore, walls of the mixing region should remain sufficiently far from the mesh nebulizer to minimize deposition.

A second primary characteristic of the small-volume mixer-heater is the use of two vibrating mesh nebulizers. A first nebulizer provides isotonic saline droplets used to humidify the airflow, while maintaining ionic balance in the lungs, and a second nebulizer provides a pharmaceutical aerosol when needed (i.e., on demand). In a *continuous mode* of operation, the humidity nebulizer runs continually and the drug nebulizer is actuated when needed during a portion of the inspiration. In *alternating mode* operation, the humidity nebulizer is paused when the drug nebulizer is actuated during a portion of each inhaled breath. While the humidity nebulizer is off, water in the drug formulation is used to humidify the airstream. Based on analytic estimates in the Results section, the nebulizers in this study are operated in alternating mode for the aerosol drug delivery experiments described below.

Based on our previous studies,[12,13] it was determined that a heating section with a rectangular (or elliptical) cross-section was ideal for warming and evaporating a nebulized aerosol. Tubular heating configurations required unreasonable lengths, resulting in increased volume and aerosol deposition. The rectangular cross-section design slows the airflow and simultaneously provides a large surface area for heat transfer. Based on the results of Longest et al.,[12] a channel height (minimum dimension) and length (in the direction of flow) of 0.7 and 12 cm may be acceptable for pharmaceutical vibrating mesh nebulizers with liquid outputs in the range of 0.2–0.4 mL/min. However, a longer heating section may be required to ensure full evaporation of the aerosol.

The initial small-volume mixer-heater prototype was based on previous studies, and is shown in Figure 1a with a 12-cm-long heating section (Design 1). The mixing section was based on the streamlined T-connector developed by Longest et al.,[35] which reduced depositional loss for an Aeroneb Lab mesh nebulizer (Aerogen Limited, Galway, Ireland) from 30.6% to 5.7% when operated at a flow rate of 30 LPM. This design includes a perforated plate near the 1.0 cm ventilation gas inlet to help unify the incoming airflow (but does not require that the aerosol pass through the porous plate). As with the streamlined T-connector, the exit of the mixing region extends along the top of the device, which was found to provide a minor reduction in depositional loss. The bore diameter of the initial mixing region was 2.4 cm, to be consistent with the T-connector of Longest et al.[35]

As described above, the heating section had an elliptical cross-section with a height of 0.7 cm, width of 5 cm, and length of 12 cm and ended with a streamlined taper leading to outlet tubing with a diameter of 0.635 cm. The approximate volume of the device starting at the center of the drug nebulizer was 19 mL for the remainder of the mixing section and 40 mL for the heating section, including the taper. Including an outlet tubing length of 50 cm, the total mixer-heater volume traversed by the aerosol is 75.0 mL, which is smaller than the 100 mL target volume.

Additional mixer-heaters considered in this study include an improved design with a circular inlet (Design 2) and a vertical design (Design 3), both with 16 cm heater lengths (Fig. 1b, c). As described in the Results, these designs are based on CFD and experimental analysis of the Design 1 case. Characteristics of Design 2 include a uniform inlet velocity profile, larger 3.5 cm internal diameter mixing region, and longer (16 cm) heating section. To further reduce mixer-heater depositional loss, Design 3 was also considered, which includes a 2.5 by 4.4 cm mixing region and a 90° rotation of the heating section. This arrangement is expected to minimize changes in aerosol direction before evaporation in the heating section. In contrast, the horizontal mixer-heater is expected to improve spreading of the aerosol over the heating channel.

The mixer-heater designs were produced using 3D printing as shown for Design 1 in Figure 2 with Aerogen Solo mesh nebulizers used as the separate humidity and drug sources. Specifically, the rapid prototypes were produced using an Objet®24™ printer (Stratasys, Inc., Eden Prairie, MN) and VeroWhite™ (Stratasys, Inc.) material. For cases where higher heat resistance was required, the heating section was rapid prototyped by selective laser sintering in a heat-resistant nylon material, DuraForm® PA (3D Systems, Rock Hill, SC).

### *Nebulizer control and heating system*

Actuation of the nebulizers and heating of the airstream were managed with a control unit. Considering nebulizer

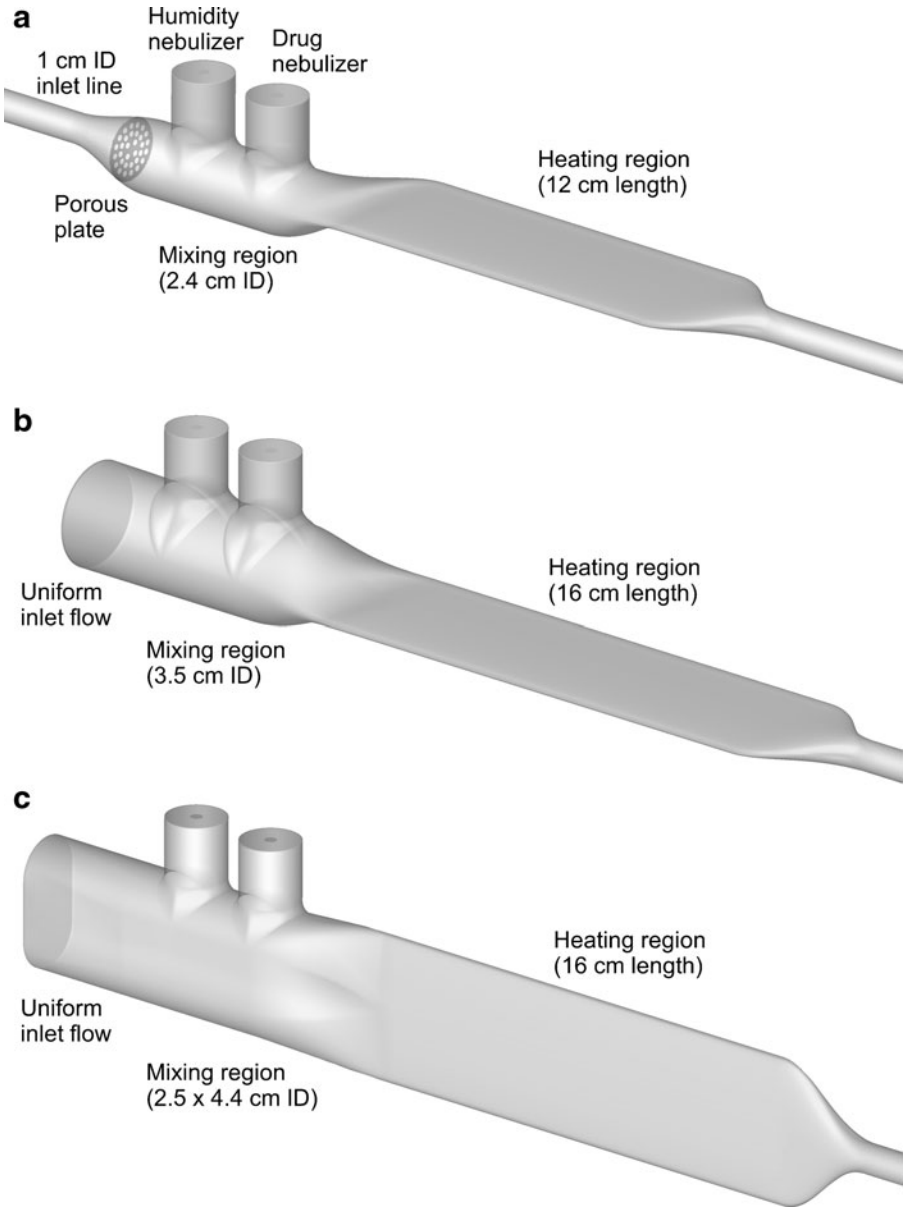


**FIG. 1.** Surface models of the mixer-heater portion of the combination HFNC and pharmaceutical aerosol device (combination device) denoted as **(a)** Design 1, **(b)** Design 2, and **(c)** Design 3. The mixer-heater is intended to produce <5% depositional loss of the nebulized dose and fully evaporate the aerosol into dried particles. HFNC, high-flow nasal cannula.

actuation, a standard Aeroneb Solo driving signal was alternated between the humidity and drug nebulizers with the switching triggered by a 50-msecond 5 V Transistor-Transistor Logic (TTL) pulse from the ASL 5000 Breathing Simulator (IngMar Medical, Pittsburgh, PA) at the start of each inhalation to initiate drug nebulization.

In this study, the nebulizers were actuated for set time periods to capture any potential transient effect of nebulizer cycling over multiple breaths. To capture a wide range of potential adult breathing conditions,[34] the drug nebulizer was actuated for a period of 1.5 seconds (approximate inhalation phase) followed by a 6-second pause in which the humidity nebulizer was actuated (approximate exhalation phase). As with conventional HFNC therapy, a constant flow rate of 20 or 30 LPM was passed through the system at all times.

The outer shell of the heating section, which is constructed in 3D printed material, contains parallel aluminum heating plates, which are heated by Kapton® (Polyimide Film) heaters (KHLV-105/5; Omega Engineering, Norwalk, CT). The two heating plates are in direct contact with the ventilation gas flow path, with the heaters positioned on the back side of the plates next to the 3D printed material, which forms an insulating layer. Approximately 1 cm from the end of the lower plate, a K-type thermocouple (SA1-XL-K; Omega Engineering) is adhered to the metal and is connected to a temperature controller (TA4; MYPIN,

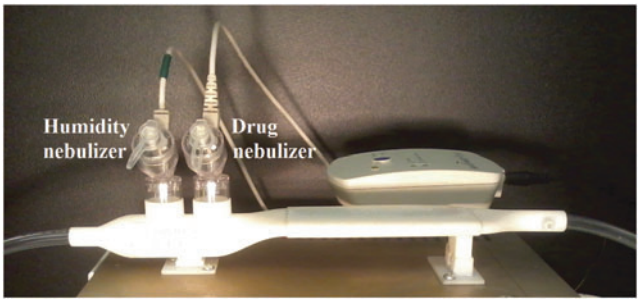


**FIG. 2.** Mixer-heater device (Design 1) produced with 3D printing and positioned on top of the nebulization and heating control unit. Separate nebulizers are used for humidifying the airstream (humidity nebulizer) and providing pharmaceutical aerosol when needed (drug nebulizer). 3D, three-dimensional.

Guangdong, China). The temperature controller regulates the heater power to attain the set point temperature at the location of the thermocouple.

A majority of the supplied energy goes into evaporating the aerosol due to the high heat of vaporization of water (~16 W) with much less energy required to heat the airstream (~5 W). Because either the humidity or drug nebulizer is active at all times, wide temperature swings in the system are avoided as the drug nebulizer cycles on and off, and the system can attain the thermocouple set point temperature in a stable manner. Preliminary experiments indicated that the initial VeroWhite material could maintain a thermocouple set point temperature of up to 60°C, but not higher due to heat damage.

### *Targeted delivery conditions*

As described in several recent reviews, HFNC therapy consists of air or blended oxygen delivered at a constant flow rate >6 LPM and typically 20 LPM and above in adults.[2,4] All modern HFNC systems heat and humidify the gas to improve patient comfort and reduce thermodynamic burden on the lungs.[2] While it is well known that heating and humidifying the airstream is required for effective HFNC therapy, the level of heat and humidity has not been objectively assessed. Lindemann et al.[24] reported human *in vivo* nasal mucosal surface temperatures measured using a rapid response miniature thermocouple at different nasal locations during inspiration and expiration. Surface temperature varied at different locations and with the breathing cycle.

The most relevant region for considering gas exposure from a nasal cannula is likely the nasal valve and anterior turbinate area. In these regions, Lindemann et al.[24] report instantaneous temperature profiles in the range of 28°C–32°C with mean (time averaged) values of 30°C–32°C. Effective HFNC therapy is intended to deliver warmed and humidified gas to the patient. Therefore, a reasonable delivery temperature consistent with the anterior nasal temperature to maintain patient comfort and provide warmed respiratory gas is assumed to be 32°C ± 2°C for this study.

Little is known regarding appropriate humidity values during all forms of NIV, in which airflow does not bypass the nose. Recommendations for invasive mechanical ventilation where the nose is bypassed are for 100% RH and 37°C, which is equivalent to 44 mg $H_2O$/liter of air (mg/L).[36] However, these delivery conditions are known to cause condensation and liquid pooling, especially in the nasal cannula and cooler (~30°C) anterior nasal regions.[23] For NIV flows, ASTM International recommends at minimum 10 mg/L of water.[37] Therefore, a reasonable goal for HFNC humidity is 10 mg/L of water vapor and above.

At temperatures of 30°C, 32°C, and 34°C, 10 mg/L of water vapor at a flow rate of 30 LPM produces RH values of 32.8%, 29.5%, and 26.5%, respectively. Therefore, our targeted RH range for HFNC therapy is approximately >30%, which provides >10 mg/L of water vapor and is larger than the ASTM International minimum required value. For perspective, 10 mg/L of water vapor delivered at 30 LPM at a room temperature of 21°C produces a RH of 55%.

In previous studies at steady-state operation and with cyclic breathing, the reservoir-based mixer-heater emitted 70%–80% of the nebulized drug dose out of the cannula.[14,15] With the advantages of the small-volume design, it is expected that the new system can achieve <10% system depositional drug loss. Optimized synchronization should enable >80% ex-cannula drug dose. It is noted that mesh nebulizers are expected to lose ~5% of the nebulized dose in the outlet skirt of the nebulizer device, which will not be altered in this study to retain the FDA-approved commercial nebulizer. Therefore, the mixer-heater device should produce ~5% or less depositional loss (based on the nebulized drug dose) to meet the <10% system depositional loss target.

### *Analytical analysis*

An analytical analysis was used to calculate exit RH at specific airflow rates and temperatures, as well as nebulizer solution concentration versus monodisperse dried particle size. Calculation of exit RH at full droplet evaporation requires knowledge of water vapor mass fraction ($Y_v$) and saturated mass fraction ($Y_{v,sat}$). The water vapor mass fraction was calculated as follows:

$$Y_v = \frac{\dot{m}_l}{\dot{m}_l + \dot{m}_{air}} \tag{1}$$

where $\dot{m}_l$ and $\dot{m}_{air}$ are the mass flow rates (g/s) of liquid water from the nebulizer and input HFNC ventilation gas, respectively. Inlet ventilation gas was at 0% RH. $Y_{v,sat}$ was determined from the Antoine equation and ideal gas law, as described by Longest and Hindle.[27] The resulting RH at a specific temperature is then calculated as follows:

$$RH = \frac{Y_v}{Y_{v,sat}} \times 100\% \tag{2}$$

The fully dried final geometric particle diameter ($d_{final}$) based on an initial droplet diameter ($d_{initial}$) is predicted as follows:

$$d_{final} = d_{initial}\left(Y_{initial}\frac{\rho_{initial}}{\rho_{final}}\right)^{1/3} \tag{3}$$

where $Y_{initial}$ is the initial total mass fraction of solutes in the nebulizer solution and $\rho$ represents initial and final densities

of the droplet or particle. In this expression, the mass fraction of drug in the solution ($Y_{initial}$) can be converted to an initial w/v ($\bar{\rho}_{initial}$) typically used in preparing formulations as follows:

$$\bar{\rho}_{initial} = Y_{initial} \cdot \rho_{initial} \quad (4)$$

where the density is entered in g/cm$^3$ and is assumed to be 1 g/cm$^3$ in this study due to the very low initial solute concentration values.

The final density ($\rho_{final}$) of the dried particle is calculated as follows:

$$\rho_{final} = \left(m_w + m_{drug} + m_{ex}\right)\left(\frac{\rho_w}{m_w + \frac{m_{drug}\rho_w}{\rho_{drug}} + \frac{m_{ex}\rho_w}{\rho_{ex}}}\right) \quad (5)$$

In this expression, $m$ and $\rho$ are the masses and densities of water ($w$), drug, and hygroscopic excipient ($ex$). The drug and model excipient considered in this study were albuterol sulfate (AS; $\rho_{drug} = 1.340$ g/m$^3$) and sodium chloride (NaCl; $\rho_{ex} = 2.160$ g/m$^3$). The nebulized formulation was prepared with 0.5% w/v combined solutes (solids) with a 50:50 NaCl to AS weight ratio. It is noted that the analytically predicted dried particle diameter is not intended to exactly match the CFD predictions or *in vitro* measurements of final size, but instead provides a theoretical minimum size that can be achieved if full drying of the aerosol occurs.

### *Computational fluid dynamics*

CFD simulations were used to analyze the initial small-volume mixer-heater design and to develop improved versions. For the CFD simulations, a steady-state flow rate of 30 LPM through the system was considered, which is consistent with HFNC therapy in adults. At this flow rate, the Reynolds number range within the initial geometry is 300–4060, indicating laminar, transitional, and turbulent flows. The simulations captured the flow field, heat transfer from the heating plates, mass transfer of water vapor, droplet transport and evaporation with a hygroscopic solute, and droplet/particle deposition. Droplet evaporation was limited by the amount of available heat and air, making two-way coupled simulations necessary.[27,38] The equations governing mass, momentum, and energy conservation, including the effects of turbulence and two-way coupling, are available in previous studies.[30,39,40] To model turbulence, the Reynolds-averaged two-equation low Reynolds number (LRN) k-$\omega$ model with shear flow corrections was implemented.[41]

Droplet and particle transport were simulated using the Lagrangian tracking approach and included terms for discrete element drag, sedimentation, and buoyancy.[42] Droplet evaporation included the effect of the solute on the droplet surface mass fraction of liquid. A complete description of droplet transport and evaporation is provided in our previous studies.[27,30] Previous studies describing two-way coupled simulations of droplet evaporation and condensation include Longest et al.[12,27,43] In these studies, an iterative approach is used between the flow solver and discrete element solver until convergence of the two-way coupling is achieved. However, in this system, the use of completely dry inlet gas caused the two-way coupling to become unstable. As a result, the droplet tracking algorithm was updated to limit the evaporation in each CFD control volume to the amount of water vapor the control volume could hold. This approach dramatically improved stability and convergence of the two-way coupling approach. Turbulent dispersion of droplets was predicted using an eddy interaction model. Anisotropic corrections for near-wall turbulence were employed as previously described.[44,45]

The commercial CFD package Fluent 16 (ANSYS, Inc.) was employed to solve the governing equations in all cases considered. User-supplied Fortran and C programs were implemented for the calculation of initial flow and droplet profiles, hygroscopic droplet evaporation, near-wall anisotropic turbulence approximations, near-wall particle interpolation,[46] as well as heat and mass sources and sinks during two-way coupling. CFD best practices were employed, including the use of second or higher order discretization, hexahedral grids,[47] and double precision calculations. Grid-converged results based on negligible change in the velocity and temperature fields (<1% relative error) as well as negligible differences in the outlet droplet size (<5%) and deposition (<5%) were established for meshes consisting of ~760,300 to 840,000 hexahedral control volumes for the small-volume mixer-heater geometries.

Inlet velocity profiles in each of the prototypes considered were consistent with a 30 LPM steady-state flow rate. Initial *in vitro* measurements confirmed that the incoming ventilation gas (medical grade air) entered the mixer-heater at ~24°C and 0% RH. In the mesh nebulizer, droplets are emitted from a 4 mm diameter mesh at a rate of ~0.4 mL/min. The resulting high-concentration droplet stream affects the momentum of the surrounding gas creating a two-way momentum coupled system. Simulating two-way momentum coupling is extremely time intensive.[48]

As a previously developed approximation,[48] a small amount of air was injected at the 4 mm mesh within the nebulizer to approximate this momentum coupling effect. The injected air had a temperature of 21°C and RH of 100%, which are typical conditions in areas of high droplet concentration and largely eliminate the thermodynamic effect of the injected air. The injected air velocity was based on high-speed video images of the aerosol plume exiting the mesh nebulizer, as reported in the Results section. The validity of this approximation will be assessed through comparison of the CFD result with *in vitro* experiments for droplet deposition, evaporation, and exiting thermodynamic conditions.

Walls of the mixer-heater geometry not including the heating surfaces were assumed to be insulated (zero heat flux) and dry (zero water vapor mass flux). The heating surfaces were set to a constant temperature based on the assumption that the aluminum plates evenly distributed the energy from the film heaters.

### In vitro—*general*

*In vitro* experiments were used to evaluate both the initial and improved small-volume mixer-heater designs at flow rates of 20 and 30 LPM. These experiments included determination of outlet temperature and RH during cyclic operation of the device, determination of aerosol depositional drug loss within

the device, and determination of the outlet aerosol particle size distribution at the exit of the mixer-heater. A rapid prototyped version of the initial mixer-heater (Design 1) is provided in Figure 2, which shows the humidity and drug nebulizers. The drug nebulizer is positioned nearest to the heating section, to minimize aerosol travel distance (device volume) and therefore maximize delivery of the more valuable medication.

In all cases, the drug nebulizer was filled with a 0.25% w/v AS and 0.25% w/v NaCl in water (0.5% w/v total solute concentration) nebulizer formulation. The humidity nebulizer was filled with isotonic saline (0.9% w/v NaCl in water). The system was typically operated with the humidity nebulizer on for 3 minutes to allow for heater warm-up and stabilization. After the 3-minute warm-up period, the system was operated in alternating mode with the drug nebulizer actuated for 1.5-second increments followed by 6.0-second increments of the humidity nebulizer.

#### In vitro—*gas temperature and RH*

Ventilation gas temperature (T) and RH were measured at the outlet of the mixer-heater for the alternating operation mode at flow rates of 20 and 30 LPM. To capture exiting energy and humidity, a custom shell was prototyped to fit around the temperature and humidity probe tip (HM70; Vaisala, Woburn, MA), and the shell positioned the probe tip parallel with the outlet of the mixer-heater. Temperature and RH measurements were recorded over a 5-minute period after the initial 3-minute startup period and time-averaged values were calculated.

#### In vitro—*depositional drug loss and aerosol particle size distribution*

Both the depositional drug loss within the mixer-heater and aerodynamic particle size distribution of drug aerosols at the outlet were determined using the alternating mode at system flow rates of 20 and 30 LPM. The drug deposition study was performed with a low resistance filter (Pulmoguard II™; Queset Medical, North Easton, MA) positioned at the exit of the mixer-heater, which was connected to a vacuum pump (30 LPM) to allow for total capture of the emitted aerosol for mass balance purposes. The aerodynamic particle size distribution was measured by replacing the filter with an Andersen Cascade Impactor (ACI, Nottingham, United Kingdom) operated at 30 LPM.

Particle sizing experiments were performed in a controlled temperature and humidity environment to prevent evaporation or condensation of the emitted aerosol before sizing in the impactor. The impactor was placed in a controlled temperature and humidity chamber and allowed to equilibrate before each experiment. The environmental conditions were set to the measured equilibrium temperature and humidity of the emitted aerosol (determined above and shown in Table 5).

In both studies, the drug nebulizer was actuated 60 times to ensure reliable dose collection. The apparatus was disembled after each run and AS was collected by rinsing the outlet skirt of the drug nebulizer, mixer-heater, and filter or ACI plates with known amounts of deionized water. The drug nebulizer was weighed before and after the experiment to calculate the nominal delivered dose. Samples were analyzed with a validated high-performance liquid chromatography (HPLC) method.

#### In vitro—*inlet velocity and heating plate temperature measurements*

Mixer-heater inlet velocity was obtained using a custom-made pitot tube assembly to relate differential pressure to air velocity. A 14-gauge needle, attached to the high-side port of a Sensirion SDP600-500 Pa pressure sensor, was placed parallel to the flow direction and was attached to a linear traversing system for positioning. Needle tip positions for the different diameter inlets (2.4 vs. 3.5 cm) were calculated based on a 6-point log-Tchebycheff method of air flow testing. The inlet sections for Designs 1 and 2 were printed to the start of the vertical plane at the beginning of the first nebulizer to allow for pitot tube positioning. Pressure readings were taken every 0.016 seconds at each point over an approximate 4-second window before moving to the next location. The average differential pressure readings at each location were used to calculate the local inlet velocity.

During device development, the heating region was thermally imaged and monitored with a Fluke Ti25 handheld infrared camera and Smartview 4.3 analysis software (Everett, WA). Heating units used for thermal imaging had rectangular sections of the 3D printed shell removed for direct imaging of the heater plate metal surface.

#### *Method summary*

Figure 3 provides an overview of the three assessment methods that were employed (analytical, *in vitro*, and CFD) and highlights the characterization metrics from each method. Metrics that were assessed from multiple methods are shown in the overlap regions and are compared in the Results section. The three assessment methods were first applied to Design 1 (initial design), which was developed based on insights from previous studies. Knowledge gained from this analysis was then used to develop Designs 2 and 3, which in combination with heating modifications to Design 1 were then analyzed using *in vitro* experiments and CFD simulations.

## Results

#### *Preliminary experimental data*

Preliminary experiments were conducted to collect necessary data for the initial analytical and CFD analyses. Liquid nebulization rates of three new Aeroneb Solo nebulizers tested three times each were determined on a gravimetric basis. The nebulizers were filled with 2 mL of a 0.9% w/v NaCl in water solution and operated for 5 minutes. The mean (standard deviation; SD) liquid nebulization rate was 0.4 (0.02) mL/min. The speed of the aerosol plume exiting the Aeroneb Solo device at a position $\sim$2 cm from the mesh (just below the nebulizer outlet flange) was determined using high-speed video recordings. The aerosol plume velocity was $\sim$3.8 m/s; however, establishing variability was difficult due to inherent transient oscillations.

The droplet diameter exiting the Aeroneb Solo device was predicted using the ACI operating with near 100% RH air to prevent droplet evaporation, as previously described.[35] The resulting mean mass median aerodynamic diameter (MMAD) of the initial Aeroneb Solo aerosol was 5.3 (0.1) $\mu$m with a geometric SD of 2.2 (0.4) $\mu$m.

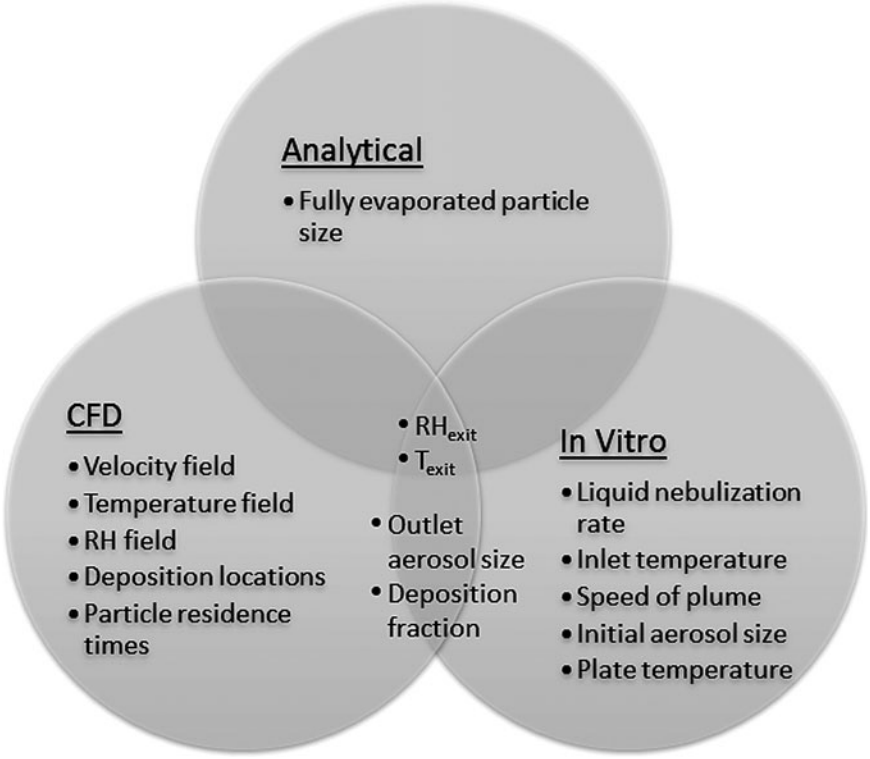


**FIG. 3.** Diagram illustrating the three assessment methods (analytical, CFD, and *in vitro* experiments), characterization metrics (e.g., outlet aerosol size), and overlap among the methods. Characterization metrics arising from more than one method (e.g., $RH_{exit}$) are compared in the Results section. CFD, computational fluid dynamics; RH, relative humidity.

### *Analytical analysis*

Table 1 provides analytically predicted outlet RH values assuming full evaporation of the aerosol and no depositional loss for specified outlet temperatures based on Eqs. (1 & 2). As described, the target outlet thermodynamic conditions for the mixer-heater are 32°C ± 2°C with RH values >30%. Actuation of one nebulizer is consistent with alternating mode delivery, and actuation of two nebulizers is consistent with continuous mode delivery during the period when both nebulizers are operating. For all cases considered, the targeted RH condition of >30% is achieved (Table 1). Lowest RH conditions occur for alternating delivery at 30 LPM, and were in the range of 35%–50%. Continuous operation at 20 LPM leads to fully saturated conditions (RH = 100%), indicating that the droplets would not completely evaporate. In contrast, RH in the range of 70%–97% can be achieved with two nebulizers (continuous mode) operating at 30 LPM. As a result, the system is capable of providing a range of RH conditions for patient comfort and can easily attain the minimum requirement of >30% RH. Operating at an outlet temperature of 32°C in alternating mode appears ideal with RH conditions at 20 and 30 LPM of 58.6% and 39.3%, respectively. As a result, analysis in the remainder of this study will focus on alternating mode operation of the nebulizers. Furthermore, a wide range of RH conditions can be achieved with the two nebulizer design if higher RH values are required in future applications.

Table 1. Analytical Predictions of Relative Humidity (%) if All Nebulized Liquid Is Evaporated for Specified Outlet Temperatures, Number of Nebulizers, and System Airflow Rates

| *Outlet temperature (°C)* | *No. of nebulizers* | *20 LPM % RH* | *30 LPM % RH* |
|---|---|---|---|
| 28 | 1 (Alternating) | 73 | 49 |
| 30 | 1 (Alternating) | 65 | 44 |
| 32 | 1 (Alternating) | 59 | 39 |
| 34 | 1 (Alternating) | 53 | 35 |
| 28 | 2 (Continuous) | 100[a] | 97 |
| 30 | 2 (Continuous) | 100[a] | 86 |
| 32 | 2 (Continuous) | 100[a] | 78 |
| 34 | 2 (Continuous) | 100[a] | 70 |

[a]Values limited to 100% indicate the occurrence of a partially evaporated aerosol.

LPM, liters per minute; RH, relative humidity.

Estimates of the fully dried (final) geometric and aerodynamic particle diameters are presented in Table 2, based on an initially measured droplet MMAD of 5.3 $\mu$m, over a range of drug nebulizer formulation total solute concentrations containing a 50:50 mixture of AS:NaCl. With the 0.5% w/v solute concentration used in the experiments, complete drying of the droplets will result in a final geometric diameter of 0.77 $\mu$m, which equates to a final aerodynamic diameter of $\sim$1 $\mu$m (calculated particle density of 1.650 g/m$^3$).

Table 2. Solute Concentration (% w/v) for the 50:50 Drug Nebulizer Mixture of AS:NaCl Versus Dried Particle Size and Drug (AS) Delivery Rate for Initial Monodisperse 5.3 μm Nebulized Droplets

| *Solute concentration (w/v) %* | *Initial droplet diameter ($d_{initial}$; μm)* | *Final geometric diameter ($d_{geo}$; μm)* | *Final aerodynamic diameter ($d_{ae}$; μm)* | *Drug mass delivery rate (μg/min)* |
|---|---|---|---|---|
| 0.001 | 5.3 | 0.10 | 0.12 | 2 |
| 0.005 | 5.3 | 0.17 | 0.21 | 10 |
| 0.01 | 5.3 | 0.21 | 0.27 | 20 |
| 0.05 | 5.3 | 0.36 | 0.46 | 100 |
| 0.1 | 5.3 | 0.45 | 0.58 | 200 |
| 0.5 | 5.3 | 0.77 | 0.99 | 1000 |
| 1 | 5.3 | 0.97 | 1.24 | 2000 |
| 5 | 5.3 | 1.65 | 2.13 | 10,000 |

AS, albuterol sulfate; NaCl, sodium chloride.

### *CFD analysis of the initial design*

CFD simulations of the initial small-volume mixer-heater design are shown in Figure 4 for a gas flow rate of 30 LPM and heating plate temperature of 60°C, which was the maximum allowed for Design 1 constructed in VeroWhite material. To match the measured aerosol inlet velocity at the outlet of the nebulizer, a 3.8 m/s inlet velocity with 100% RH air stream was applied to the 4 mm diameter nebulizer mesh. Applying the injected air velocity over the 4 mm mesh resulted in an additional flow of 2.9 LPM through the system, which is <10% of the total flow for the CFD simulation (30 LPM ventilation gas inlet) and not sufficient to appreciably change the heat transfer characteristics of the downstream region.

Midplane and cross-sectional contours of velocity and velocity stream traces indicate nonuniform flow in the mixing region, which is initiated at the porous inlet plate (Fig. 4a). Recirculation is observed to occur in the nebulizer body and downstream of the junction between the drug nebulizer and mixer-heater. Temperature contours indicate rapid heating of the inlet 24°C air; however, the mixer-heater outlet temperature of 29°C is lower than the targeted value of 32°C (Fig. 4b) at the initial maximum plate temperature of 60°C. Particle trajectories do not sufficiently spread over the heating channel (laterally normal to the direction of flow); however, near-full evaporation of the aerosol is achieved with an outlet MMAD of 0.9 μm (Fig. 4c).

Predicted total aerosol particle deposition within the nebulizer skirt and mixer-heater was 20.2% of the nebulized dose, with significant concentrations of deposited drug particles in the transition region at the heater inlet and near the heater outlet (Fig. 4d). Based on the approximate inlet condition used to capture momentum from the mesh nebulizer, it was not possible to accurately differentiate between deposition in the nebulizer skirt and mixer-heater.

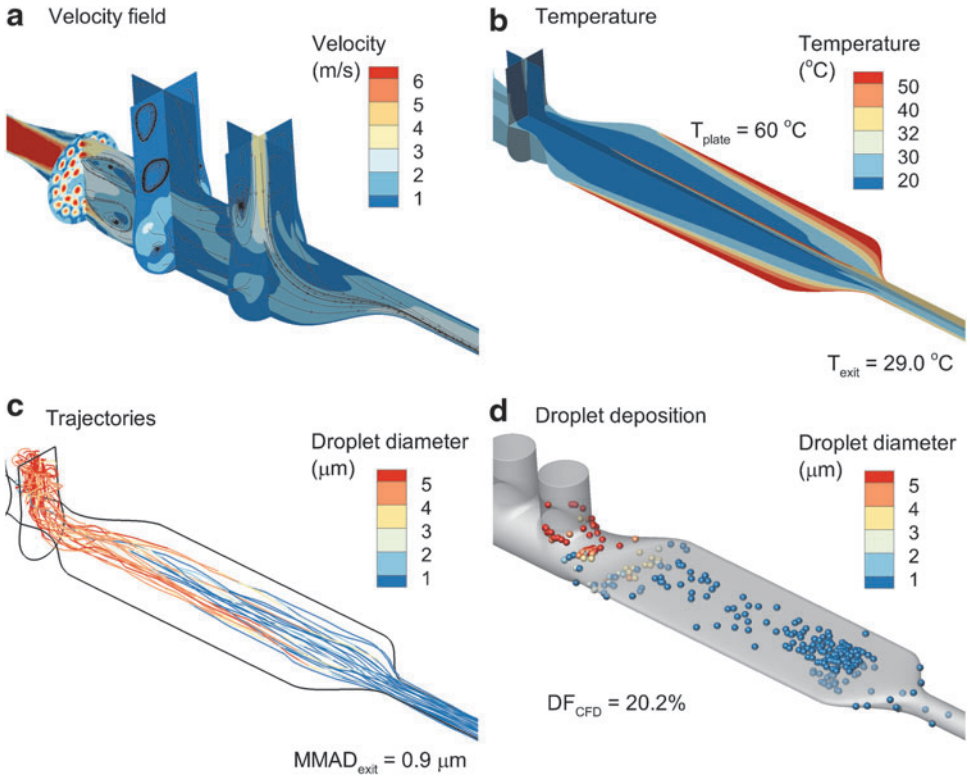


**FIG. 4.** CFD analysis of Design 1 operated at 30 LPM with a constant plate temperature of 60°C, including **(a)** surface contours and stream traces of the velocity field, **(b)** contours of the temperature field, **(c)** droplet trajectories with an initial size of 5.3 μm and colored based on geometric diameter, and **(d)** droplet deposition locations, including the size of the droplets/particles at the point of deposition. LPM, liters per minute.

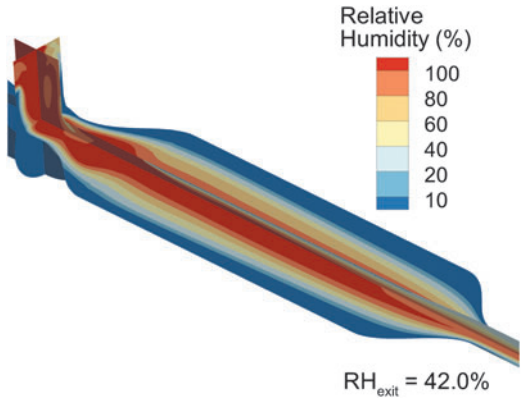


**FIG. 5.** RH field of Design 1 producing an outlet RH of 42% with an outlet temperature of 29°C.

Contours of RH, including the effect of the evaporating aerosol on the thermodynamics of the gas stream (with two-way temperature and mass coupling), are shown in Figure 5. At 30 LPM, the mass-flow-weighted average RH of 42% at 29°C is similar to the analytically predicted range in Table 1, giving confidence in the CFD model predictions. However, the CFD-predicted value is ~10% (relative difference) lower than the analytical prediction due to some aerosol depositional loss occurring in the model when unevaporated droplets hit the geometry walls. In the CFD calculations, particles are removed from the flow field at the time of particle-to-wall contact and further contribution of water vapor mass to the flow field is not considered.

### In vitro *analysis of the initial prototype*

Experimentally measured temperature and RH values for Design 1 with a 60°C thermocouple temperature are shown in Table 3 for alternating mode delivery. Measured RH values at 20 and 30 LPM are ~10% (relative difference) below analytically predicted values, likely because of aerosol depositional loss occurring with the experimental system. Agreement between the experimental and CFD-predicted values at 30 LPM is excellent for both temperature (28.7°C vs. 29.0°C) and RH (40.3% vs. 42.0%). As observed with the CFD analysis, the desired outlet temperature of 32°C was not attained in the experiments with a plate thermocouple temperature of 60°C. With Design 1 and VeroWhite material, increasing the thermocouple temperature above 60°C resulted in heat damage to the system.

Table 3. Experimentally Measured Mean (Standard Deviation) Temperature and Relative Humidity Values for Design 1 with a 60°C Thermocouple Temperature Operating in Alternating Mode

| | *20 LPM* | *30 LPM* |
|---|---|---|
| Initial_12 cm | | |
| T (C) | 26.6 (0.1) | 28.7 (0.2) |
| RH (%) | 61 (0.6) | 40 (0.8) |

T, temperature.

Experimentally measured aerosol deposition fractions (as a percent of nebulized dose) and the MMAD exiting the mixer-heater for Design 1 and a 60°C plate temperature are reported in Table 4. Experimental determinations of depositional loss in the mixer-heater at both flow rates are ~11%. Combining the nebulizer and mixer-heater deposition fractions at 20 and 30 LPM, respectively, results in total depositional loss values of 19.3% and 17.3%.

In comparison, the combined deposition fraction (DF) from CFD at 30 LPM was 20.2%, indicating good agreement with the experimental system. As described, depositional drug losses in the mixer-heater are considerably higher than the desired 5% or less target values. Moreover, the experimental measurements also indicate incomplete evaporation of the aerosol, with an exit MMAD of 1.7 $\mu$m at 20 LPM and 1.6 $\mu$m at 30 LPM. The CFD model underpredicted the exiting aerosol size in comparison with the experiments.

### In vitro *optimization and design improvements*

Both CFD simulations and experiments identified shortcomings of Design 1 to be low exit temperature and depositional drug loss that was higher than targeted. Depositional losses in the mixing region were associated with nonuniform inlet flow and disturbed flow patterns. It was expected that these flow patterns and associated depositional drug losses could be reduced by (1) unifying the inlet flow and (2) increasing the mixing region diameter to 3.5 cm. To improve the inlet flow profile, a flow unifier was developed as described below.

To verify nonuniform inlet flow as observed with CFD, the pitot tube velocity measurement probe tip was traversed across the inlet porous plate of Design 1 at an offset distance of 1.4 cm corresponding to immediately upstream of the humidity nebulizer. Sample velocity traces in Design 1 operated at 30 LPM are shown in Figure 6a with maximum and minimum flow rate differing by a ratio of 15.5:1. These velocity traces were taken on horizontal and vertical lines (with respect to gravity) on the same axial plane. To unify the inlet velocity profile within a compact volume, a 3D mesh of rods was developed (Fig. 6b). The rods had a diameter of 1.75 mm with an in-plane gap distance of 1.0 mm and were contained centrally on 2-mm-thick circular inserts with each insert rotated by 90°. Six circular inserts ending in a filter media insert (Pulmoguard II; Queset Medical) were used to construct the flow unifier. As shown in Figure 6a, the

Table 4. Experimentally Determined Mean (Standard Deviation) Aerosol Deposition Fraction (% of Nebulized Dose) in Different Regions for Design 1 with a 60°C Thermocouple Temperature and Mean (Standard Deviation) Mass Median Aerodynamic Diameter of the Outlet Aerosol

| | *20 LPM* | *30 LPM* |
|---|---|---|
| Design 1 | | |
| Nebulizer (%) | 8.1 (0.2) | 6.1 (0.8) |
| Mixer-heater (%) | 11.2 (0.6) | 11.2 (1.5) |
| Outlet filter (%) | 78.0 (1.9) | 76.6 (0.4) |
| MMAD ($\mu$m) | 1.7 (0.1) | 1.6 (0.0) |

MMAD, mass median aerodynamic diameter.

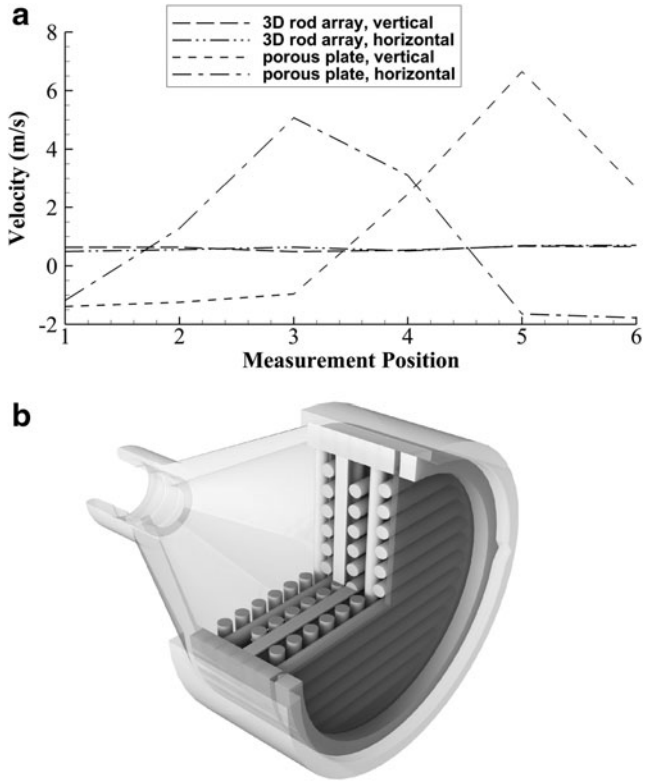


**FIG. 6.** Development of the inlet flow unifier device, including **(a)** sample inlet velocity profiles in horizontal and vertical directions without (Design 1) and with (Design 2) the flow unifier, **(b)** assembled Design 2 flow unifier, including a Pulmoguard II™ (Queset Medical, North Easton, MA) filter at the outlet.

flow unifier reduced maximum to minimum inlet velocity difference ratios to a value of 1.9:1.

The limitations of low exit temperature and incomplete aerosol evaporation are interconnected and may be the result of poor aerosol spreading over the heating section. To improve heat transfer, the heating section length was increased to 16 cm. Furthermore, it was not clear how the thermocouple temperature differed from the plate temperature field under flow conditions. A thermal image of the heating section for Design 1 with the plate operated at a thermocouple temperature of 60°C and flow rate of 30 LPM is shown in Figure 7. The heated plate is observed to have a highly variable temperature profile with visible temperatures ranging from 59°C to 73°C.

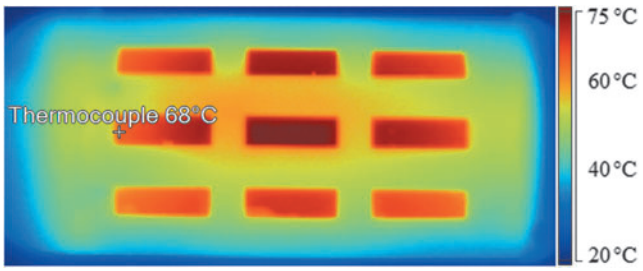


**FIG. 7.** Thermal image of the heating plate taken with rectangular sections of the outer nylon shell removed for the Design 1 mixer-heater operated at 30 LPM with a thermocouple set point temperature of 60°C. Approximate thermocouple location marked and labeled with software-determined temperature.

To improve the heating conditions, two approaches were taken. First, the heating section was constructed from a heat-resistant nylon material (DuraForm PA; 3D Systems) that could withstand the higher operating temperatures near the heater strips. Second, the thermocouple temperature was considered to be an adaptable set point for each mixer-heater to achieve the desired outlet temperature of 32°C ± 2°C. Based on experimental measurements, the thermocouple set points to achieve steady-state outlet temperatures of 32°C ± 2°C for Design 1, Design 2, and Design 3 were 93°C, 110°C, and 134°C, respectively for 30 LPM airflow. It is noted that these set point thermocouple temperatures are related to the position of the thermocouple on the heating plate as well as design of the heating plates. Therefore, the set point temperatures do not necessarily represent the average plate temperature.

### *CFD development and analysis of the improved mixer-heater designs*

CFD analysis of the Design 2 mixer-heater is shown in Figure 8. Velocity fields and stream traces show significantly less recirculation in the mixing region, as expected, together with enhanced transport toward the lower heating plate (Fig. 8a). Uniform inlet flow and the increased heating length improve effectiveness of the heating region, resulting in an outlet temperature of 32.4°C for a uniform wall temperature of 55°C. Surprisingly, Design 2 spreads the aerosol over the entire width of the heating section, resulting in full evaporation of the aerosol and an outlet MMAD of 1.0 $\mu$m (Fig. 8c). The associated CFD-predicted total depositional loss (nebulizer and mixer-heater) is 10.6%, which is just above the 10% total target, but could potentially be even lower if deposition in the transition between the mixer and heater regions was reduced (Fig. 8d).

To further reduce depositional loss, Design 3 was developed as shown in Figure 9. A flow unifier was also developed for Design 3 such that the CFD boundary condition was again uniform inlet flow. While streamlines are highly linear, the heat transfer region was less effective with a 60°C constant wall temperature required to produce an outlet temperature of 31.5°C (Fig. 9b). Trajectories illustrate a concentration of the aerosol along the top half of the vertical heating region, resulting in incomplete evaporation (MMAD = 1.1; Fig. 9c). However, the CFD-predicted total depositional loss (nebulizer and mixer-heater) was further decreased to 9.9%.

As described, all three geometries have volumes below the 100 mL target (including 50 cm of outlet tubing). However, trajectories and turbulence result in different mean droplet transit times through the mixer-heater, as shown in Figure 10. Each design has a mean transit time of <0.3 seconds, as desired. Design 2 increases droplet transit time from 0.23 to 0.27 seconds. However, due to flow streaming through the middle and top half as well as reduced turbulence, Design 3 has the fastest average droplet transit time ($t_{exit}$ = 0.18 seconds; Fig. 10c).

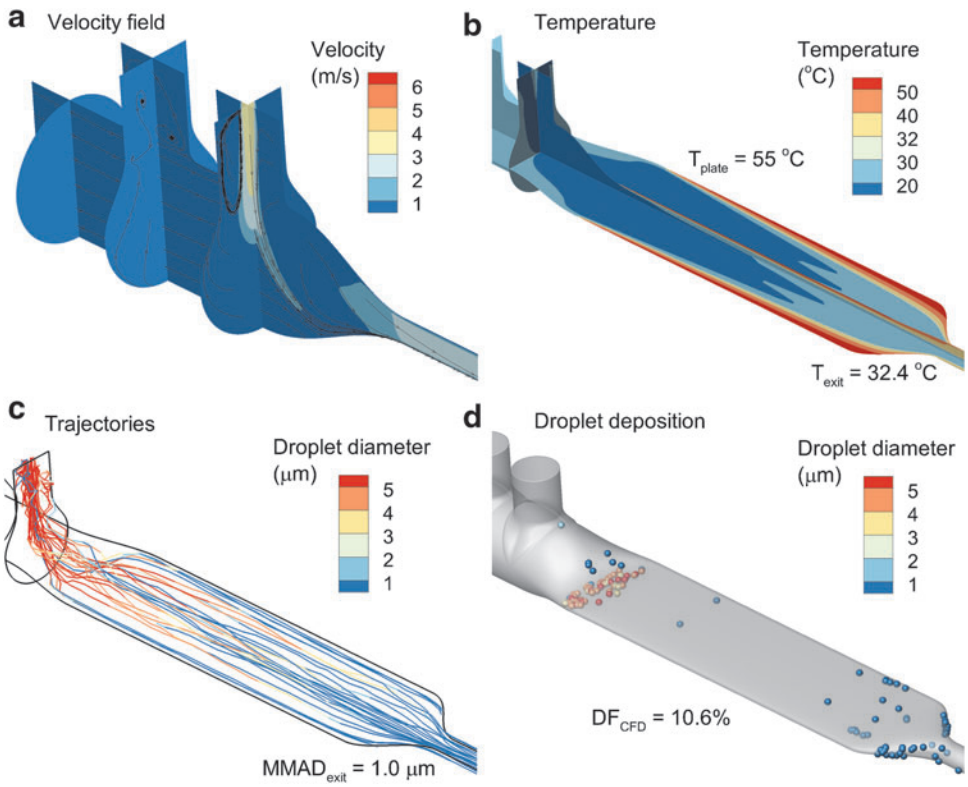


**FIG. 8.** CFD analysis of Design 2 operated at 30 LPM with a constant plate temperature of 55°C, including **(a)** surface contours and stream traces of the velocity field, **(b)** contours of the temperature field, **(c)** droplet trajectories with an initial size of 5.3 $\mu$m and colored based on geometric diameter, and **(d)** droplet deposition locations, including the size of the droplets/particles at the point of deposition.

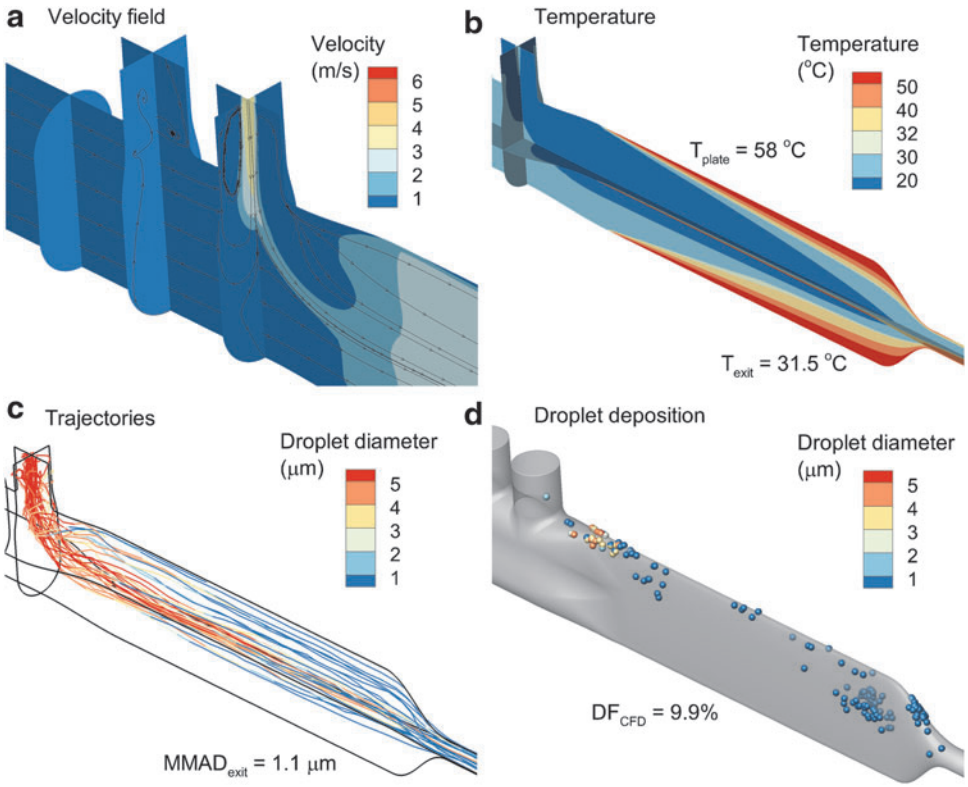


**FIG. 9.** CFD analysis of Design 3 operated at 30 LPM with a constant plate temperature of 60°C including **(a)** surface contours and stream traces of the velocity field, **(b)** contours of the temperature field, **(c)** droplet trajectories with an initial size of 5.3 $\mu$m and colored based on geometric diameter and **(d)** droplet deposition locations including the size of the droplets/particles at the point of deposition.

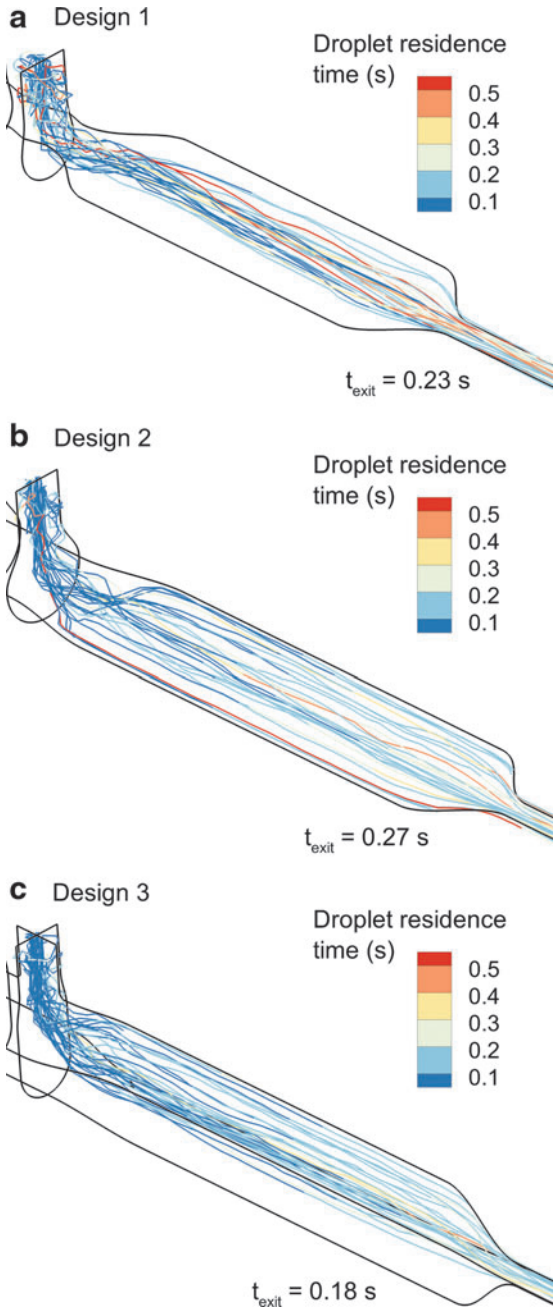


**FIG. 10.** Droplet trajectories contoured by mixer-heater residence time (starting at the point of injection from the drug nebulizer) for **(a)** Design 1, **(b)** Design 2, and **(c)** Design 3.

### *Experimental analysis of improved designs*

For experimental testing, the heating sections of all three designs were produced in heat-resistant DuraForm™ nylon resin. Set point temperatures of the heating plates in each design were adjusted to achieve an outlet temperature of 32°C ± 2°C after the 3-minute warm-up period. Experimentally measured temperature and RH conditions at the outlet of each heater system are reported in Table 5. In all cases, the target outlet temperature of 32°C ± 2°C was achieved. Measured RH conditions were consistently lower than predicted with the analytical model. Specifically, at 20 and 30 LPM, measured RH was 40% and 20% below (relative difference) analytically predicted values, respectively. Furthermore, measured RH conditions were similar between 20 and 30 LPM cases.

Theoretically, RH conditions at 20 LPM should be larger than at 30 LPM by a factor of 1.5-fold, assuming similar depositional losses among the cases. As a final observation, RH values are expected to be similar between designs at a constant flow rate, assuming similar depositional losses, as was seen at 30 LPM. However, larger variations in RH values are observed at 20 LPM, with Design 2 having the highest RH and Design 1 having the lowest RH. These unexpected RH findings may arise from difficulty in measuring water vapor content in a fast moving heated gas stream that also contains a hygroscopic aerosol, which may potentially deposit and collect on the RH probe.

Experimentally determined deposition fractions and MMADs of the aerosols exiting the three systems are reported in Table 6. Depositional loss was reasonably

TABLE 5. EXPERIMENTALLY MEASURED MEAN (STANDARD DEVIATION) TEMPERATURE AND RELATIVE HUMIDITY VALUES FOR ALL MIXER HEATER DESIGNS WITH A TARGETED 32°C OUTLET TEMPERATURE OPERATING IN ALTERNATING MODE

| | *20 LPM* | *30 LPM* |
|---|---|---|
| Design 1 | | |
| T (C) | 32.7 (0.5) | 32.2 (0.6) |
| RH (%) | 33 (2.1) | 32 (1.7) |
| Design 2 | | |
| T (C) | 32.8 (0.5) | 32.0 (0.7) |
| RH (%) | 39 (1.1) | 30 (0.0) |
| Design 3 | | |
| T (C) | 32.7 (0.3) | 32.4 (0.5) |
| RH (%) | 35 (0.6) | 30 (1.1) |

TABLE 6. EXPERIMENTALLY DETERMINED MEAN (STANDARD DEVIATION) AEROSOL DEPOSITION FRACTION (% OF NEBULIZED DOSE) IN DIFFERENT REGIONS OF ALL MIXER-HEATER DESIGNS WITH A TARGETED 32°C OUTLET TEMPERATURE AND MEAN (STANDARD DEVIATION) MASS MEDIAN AERODYNAMIC DIAMETER OF THE OUTLET AEROSOLS

| | *20 LPM* | *30 LPM* |
|---|---|---|
| Design 1 | | |
| Nebulizer (%) | 7.0 (0.7) | 9.1 (0.7) |
| Mixer-heater (%) | 11.4 (1.2) | 11.1 (0.6) |
| Outlet filter (%) | 71.1 (2.4) | 71.2 (0.4) |
| MMAD ($\mu$m) | 1.2 (0.1) | 1.2 (0.0) |
| Design 2 | | |
| Nebulizer (%) | 7.2 (0.7) | 7.0 (1.4) |
| Mixer-heater (%) | 6.2 (1.6) | 4.5 (1.6) |
| Outlet filter (%) | 79.2 (4.1) | 80.2 (3.4) |
| MMAD ($\mu$m) | 1.3 (0.1) | 1.2 (0.1) |
| Design 3 | | |
| Nebulizer (%) | 9.3 (1.6) | 9.2 (3.9) |
| Mixer-heater (%) | 4.4 (1.8) | 4.1 (2.4) |
| Outlet filter (%) | 80.5 (1.1) | 85.5 (4.7) |
| MMAD ($\mu$m) | 1.2 (0.2) | 1.1 (0.1) |

consistent between 20 and 30 LPM, allowing for a focus on conditions at the higher flow rate. Considering the mixer-heater, ~10% deposition in Design 1 was reduced to ~5% loss with Design 2 and <5% with Design 3.

However, in all cases, aerosol deposition in the skirt of the nebulizer was ~10%, making it not possible to achieve <10% total deposition in the system. Combining the nebulizer and mixer-heater depositional losses at a flow rate of 30 LPM, as with the CFD calculations, the system with the lowest total loss was Design 2 (11.5%) followed by Design 3 (13.3%) and then Design 1 (20.2%). A similar rank order in total depositional loss is observed at 20 LPM, but with both Design 2 and 3 having a total loss of ~13%. In all cases, the measured MMAD was within the range of 1.1–1.3 $\mu$m with a very small SD range (0–0.2) (Table 6).

### *Verification of CFD results in improved designs*

System depositional losses (nebulizer and mixer-heater) are compared between the experimental measurements and CFD predictions in Figure 11 with a targeted 32°C outlet temperature. In all cases, the CFD predictions fall within ±1 SD of the mean experimental values. As described, the CFD model could not capture the distribution of aerosol deposition between the nebulizer and mixer-heater. Nevertheless, the CFD predictions accurately captured mean total depositional loss in the system, which implies accurate predictions of system-emitted dose. In all cases, CFD-predicted MMAD values of ~1 $\mu$m were close to the measured values of 1.1–1.3 $\mu$m.

## Discussion

The improved mixer-heater prototypes, Designs 2 and 3, both met the primary challenge of 5% or less depositional loss. Surprisingly, the Aeroneb Solo mesh nebulizer had ~10% depositional loss in the nebulizer skirt region, which was higher than previously observed in other systems using the Aeroneb Lab and Pro nebulizers.[12,14,35,49] It is not clear if this increase in depositional loss is due to the nebulizer device or circulating airflow patterns arising from the cross-flow design of the mixing region. At the primary flow rate of interest (30 LPM), Designs 2 and 3 had total depositional losses (nebulizer and mixer-heater) of 11.5% and 13.3% of the nebulized dose, respectively, which are acceptably close to the target of 10% system deposition. Reducing the system flow rate to 20 LPM did not appreciably change performance. Both devices provided adequate evaporation of the aerosol, with Design 3 producing slightly more drying potential than Design 2. However, Design 3 had a substantially faster aerosol clearance time compared with Design 2. As a result, both Designs 2 and 3 performed well with respect to aerosol delivery and should be considered further in future realistic aerosol delivery testing.

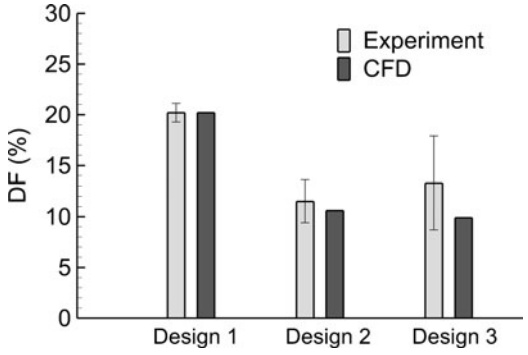


**FIG. 11.** Comparison of total deposition fractions (as a percentage of nebulized dose) within the nebulizer and mixer heater based on experimental data and CFD predictions. Three trials of each experiment were conducted ($n = 3$) and error bars denote ±1 standard deviation of the experimental data.

Considering device outlet temperature and RH measurements, producing the heating section in heat-resistant material enabled all designs to achieve the targeted temperature range of 32°C ± 2°C during aerosol production within the first 3 minutes of operation. As described, the RH results are less clear. Consistency was observed between RH measurements, analytical calculations, and the CFD predictions for the initial system (Design 1) with a plate temperature of 60°C. However, measured RH conditions were substantially lower with increased outlet temperatures, did not agree with the analytic calculations, and were not consistent with thermodynamic concepts. It is expected that the current measurement setup may not be able to capture the complete RH of the small diameter (~0.7 cm) aerosol and gas stream exiting the mixer heater. Still, measured RH values achieved the 30% target value.

For high efficiency transnasal (i.e., nose to lung) aerosol delivery, the mixer-heater is intended to evaporate a majority of the liquid from the droplets, producing an aerosol size of ~1 $\mu$m or below. These values were observed to be close to the experimentally measured MMAD values exiting the heater section, which were approximately 1.1–1.3 $\mu$m. Based on the validated CFD predictions of Walenga et al.,[50] at this aerosol size, depositional loss of ~7% is expected in a streamlined nasal cannula and average adult nasal airway combined. Similarly, CFD predictions indicate a fully dried aerosol with an MMAD of ~1 $\mu$m at the device outlet, which produces <4% depositional loss in the same streamlined nasal cannula and nasal model. The CFD predictions were based on an initial monodisperse aerosol size, but were similar when simulating the full polydisperse initial aerosol distribution. Both the experimental measurements and CFD predictions satisfy the requirement of a small aerosol with relatively little expected depositional loss.

It is noted that the analytical estimates of particle size represent a minimum that can only be achieved if complete drying of the aerosol droplets into particles occurs. Partial evaporation of the aerosol is viewed as a less controlled and likely unstable state that will be associated with low gas stream temperatures, on the order of ~21°C; therefore, full evaporation of the aerosol is desired. However, if partial evaporation of the aerosol is to be predicted analytically, then more advanced models of evaporation[38,43] that include two-way coupling are needed.

A primary advantage of using mesh nebulizers to provide both the humidity source and drug aerosol is that one constant temperature heating region can be implemented. This approach simplifies the heating control, better evaporates the aerosol, and helps to maintain a safe targeted inhalation

temperature. For example, if the HFNC gas was composed of water vapor and air (or an oxygen mixture), as with all current commercial systems, ~5 W of power would be required to heat the flow stream from 24°C to 32°C. However, during periods when the drug nebulizer is actuated, a total of 21 W of power is required to evaporate the aerosol and heat the flow stream, due to the high latent heat of vaporization of water. To provide this additional power input, the heating section would need to cycle temperature up very quickly during periods of nebulizer actuation to provide 21 W and then cycle temperature back down to provide 5 W. Considering that the drug nebulizer is only actuated for a portion of the inhalation period, which may be under 1 second, the temperature cycling of the heating section becomes difficult to control and will likely underevaporate the aerosol at the start of drug nebulization and then overheat the airstream at the end of nebulization. If 21 W of power, which is required when the nebulizer is actuated, is applied to a gas stream of air and water vapor without aerosol droplets, the outlet temperature will become ~60°C (140°F), which is not safe for direct inhalation. In contrast, the alternating nebulizer design in which both nebulizers deliver the same liquid flow rate and only one nebulizer fires at a time, allows the single heating section to remain at one constant temperature with a constant power input of ~21 W.

In developing a high efficiency aerosol administration system, it is also important to consider the drug formulation delivery rate. The Aeroneb Solo mesh nebulizer was found to nebulize an aqueous low-concentration formulation at a rate of ~0.4 mL/min. In this study, the drug aerosol nebulizer was only actuated 20% of the time (with the humidity nebulizer actuated the remaining 80% of the time). Considering the estimated 90% aerosol delivery efficiency, the resulting delivery rate of the drug formulation out of the combination device was 0.072 mL/min. During deep inspiration, the drug delivery time may be increased to ~50%, resulting in a maximum drug formulation delivery rate (assuming 90% delivery efficiency) of 0.18 mL/min. Increases in the nebulization rate are also allowable by as much as twofold considering that the RH of the heated aerosol stream was ~30% at a flow rate of 30 LPM.

A number of other studies have evaluated aerosol delivery efficiency during HFNC therapy. Using commercial components and Aerogen mesh nebulizers, estimated lung doses are typically either less than ~5% for small diameter nasal cannula[9,51,52] or less than ~15% for larger diameter adult nasal cannula.[11,53] These previous studies have seldom reported depositional losses in the delivery system separate from lung delivery efficiency. One exception is the *in vivo* study of Dugernier et al.,[10] who considered mesh nebulizer aerosol delivery during HFNC therapy using single-photon emission computed tomography in humans. Total depositional loss in the delivery system was 58.2% of the nebulized dose with only 3.6% reaching the lungs. Assuming small tubing and nasal cannula deposition, based on small particles and streamlined designs,[50] the mixer-heater in this system is approximately five to six times more efficient than the commercial system evaluated by Durgernier et al.[10]

The transnasal pulmonary aerosol delivery (tPAD) device considered by Zeman et al.[54] does not report device delivery efficiency, but includes a ''spacer'' to selectively filter larger droplets from an Aerogen Pro mesh nebulizer, with an estimated delivery rate of 0.4 mL/min[13] when actuated continuously. From the reported ex-device delivery rate of 2 mL/h (or 0.033 mL/min),[54] it can be estimated that the tPAD device has a delivery efficiency of ~8% of the nebulized dose. Hence, the mixer-heater device developed in this study is significantly more efficient than commercial and other experimental systems, and produces a significantly higher drug formulation delivery rate.

In this study, an EEG formulation of 50:50 AS and NaCl was employed as a test aerosol based on its safety profile and well-developed characterization methods. As described in our previous work, the EEG approach delivers a small-particle aerosol that is composed of an inhaled medication and hygroscopic excipient.[26,30] The small initial size of the aerosol provides for low depositional loss in the delivery system and extrathoracic airways. Once inside the lungs, the presence of the hygroscopic excipient causes the particles to take up water, increase in size, and deposit. The amount and type of hygroscopic excipient, initial aerosol size, and inhaled air conditions can all be used to control the rate of particle size increase and, together with inhalation rate, can be used to target the region of deposition.[28,29,43]

Considering AS and other bronchodilators delivered during NIV, clinical benefit is frequently reported even though the lung delivery efficiency is low (typically <10%) and intersubject variability is high for conventional delivery systems.[5,6,8,55,56] This is generally considered acceptable because AS has a wide therapeutic window, relatively mild side effects, and is relatively inexpensive. Nevertheless, improved knowledge of the delivered dose may help to lessen the potential beta-agonist side effects of atrial and ventricular arrhythmias and tachycardia,[7,57,58] especially when these medications are delivered in very high doses as with acute severe asthma.

Beyond the administration of bronchodilators, we envision the combination delivery device to be useful for respiratory drug delivery in cases involving (1) high-dose nebulized medications, (2) drugs with rapid absorption where continuous delivery is beneficial, (3) medications that require uniform concentration in ASL, and (4) therapeutics targeted to specific lung regions such as the tracheobronchial or alveolar airways. One potential sample application that could benefit from the combination delivery system and the EEG strategy is the administration of nebulized antibiotics, which may require high doses and would likely benefit from uniform surface concentration throughout the lungs. At the current nebulized solution concentration of 0.5%, the combination device delivers ~0.9 mg/min of drug (with deep inspiration at a liquid delivery rate of 0.18 mL/min). Increasing the solute concentration to 3% would further increase the drug delivery rate to 5.4 mg/min and would produce an ~1.9 $\mu$m (aerodynamic diameter) aerosol, which is still expected to have low extrathoracic depositional loss. Tian et al.[28] previously considered nose-to-lung delivery of 1 $\mu$m EEG particles using a complete-airway CFD model. Compared with conventional static particle sizes, the EEG approach increased small tracheobronchial airway deposition by a factor of ~35-fold.[28] This increase is approaching what is required to achieve uniform concentration in ASL ($\mu$g of drug/mL of liquid) based on initial particle deposition site.

A second application of the combination device may be continuous or long-term administration of inhaled medications, perhaps during sleep. As described by Geller,[59] beta-lactam antibiotics are effective based on the duration of time the drug concentration remains above the minimum inhibitory concentration of the bacteria, in comparison with other concentration-dependent antibiotics. The long-term administration of beta-lactams simultaneously with HFNC or other forms of NIV may provide another option for the treatment of respiratory infections that is not currently available. Zeman et al.[54] describe the tPAD device for administration of hypertonic saline to improve airway clearance in cystic fibrosis (CF) subjects. However, clinical trials did not indicate an improvement in clearance rate associated with overnight administration of hypertonic saline,[60] which was likely due to an insufficient delivery rate.[60] Based on hypertonic saline oral inhalation studies, a target delivery rate for effective improvement in clearance may be closer to 5.0 mg/min,[60] whereas the tPAD device delivered 1.3 mg/min or less using a 7% saline formulation.[60] For NaCl as the therapeutic molecule in the combination device, increasing the concentration to 3% will increase the drug delivery rate to 5.4 mg/min and the dried aerodynamic particle diameter to 1.9 $\mu$m. The increase in dried hygroscopic particle size would likely be effective in targeting the tracheobronchial region and especially the lower tracheobronchial airways. However, it is not clear if delivering dried particles with humidity, which then rehydrate before deposition, will be more or less effective compared with nebulizer delivery of standard 7% hypertonic saline for improving airway clearance. Considering a third application, the dual nebulizer setup may be useful for the administration of different therapies simultaneously, potentially targeting different regions of the lungs based on nebulizer timing, in an effort to reduce treatment time and burden for subjects with complex inhalation regimes, as with CF.

Several study limitations should be noted and addressed before advancement of the combination device to human subject testing. In this evaluation, the system lacked a nasal cannula interface, which when included will result in additional depositional losses. However, in multiple previous studies, we have described the development of streamlined nasal cannula interfaces[12,35,61] that are designed for aerosol administration and have very low depositional losses (<1% for nebulized aerosol based on *in vitro* experiments[12]) when delivering particles on the scale of $\sim$1 $\mu$m at flow rates of $\sim$30 LPM. Compared with other HFNC systems, we propose that RH values >30% (and in the range of 40%–60%) are acceptable for HFNC therapy, based on ASTM standards for NIV.[37] Moreover, by using an RH condition that is below 100%, common HFNC problems of liquid sputtering[23] and nose drippage may be avoided. The use of nebulized isotonic saline is currently untested as a means to humidify the airways on a long-term basis. We contend that delivering isotonic saline will help to maintain the correct osmotic gradient in the lungs, compared with the common practice of delivering humidity from pure water vapor. Furthermore, the salt concentration can be increased to enable simultaneous hypertonic saline administration, which is a known therapy for improving airway clearance.[62] In this study, alternating actuation of the nebulizers was simply cycled with an expected inhalation time course. In future studies, breath monitoring will be added to the system to enable active synchronization of the aerosol during a portion of inhalation. It is expected that maximum delivery efficiency can be achieved when the subject can execute a ''slow and deep'' inhalation together with active synchronization of the aerosol delivery.

Future *in vitro* studies will be conducted with variable breathing scenarios to test the ability to sense flow and synchronize actuation for a variety of nasal anatomies. *In vitro* studies are also in progress to further test safety and reliability of the heating system. Upon *in vitro* testing and development of the combination system with synchronized delivery, studies to determine the lung deposition of radiolabeled aerosol in human subjects are planned.

In conclusion, multiple approaches (analytical, *in vitro* experimental, and CFD) were used concurrently to develop a new combination device for administering HFNC therapy and simultaneous ''on-demand'' pharmaceutical aerosols to the lungs with high efficiency. Designs 2 and 3 both satisfied the 5% or less mixer-heater depositional loss requirement and produced small-particle aerosols with expected subsequent low depositional losses. Based on CFD and *in vitro* assessment of an initial design, the validated CFD model was used to guide development of the improved designs and achieve the specified performance metrics. Rapid prototyping and experimental testing of the improved designs confirmed improved aerosol and outlet temperature performance. Potential limitations of each approach were overcome with comparisons to the other methods.

Further studies are needed to verify the expected analytical predictions of RH in all cases and resolve differences between predicted and measured outlet particle size. A system for synchronizing alternating actuation of the nebulizers with inspiration is currently in development. Subsequent studies will consider lung delivery efficiency during cyclic respiration using realistic *in vitro* airway models and then human subject testing.

## Acknowledgments

Research reported in this publication was supported by the National Heart, Lung, and Blood Institute of the National Institutes of Health under Award Number R01HL107333. The content is solely the responsibility of the authors and does not necessarily represent the official views of the National Institutes of Health.

## Author Disclosure Statement

Virginia Commonwealth University is currently pursuing patent protection of devices and methods described in this study, which if licensed and commercialized, may provide a future financial interest to the authors.

## References

1. Nishimura M: High-flow nasal cannula oxygen therapy in adults. J Intensive Care. 2015;3:15.
2. Ward JJ: High-flow oxygen administration by nasal cannula for adult and perinatal patients. Respir Care. 2013;58:98–120.
3. Haq I, Gopalakaje S, Fenton AC, McKean MC, O'Brien CJ, and Brodlie M: The evidence for high flow nasal cannula devices in infants. Paediatr Respir Rev. 2014;15: 124–134.

4. Lee JH, Rehder KJ, Williford L, Cheifetz IM, and Turner DA: Use of high flow nasal cannula in critically ill infants, children, and adults: A critical review of the literature. Intensive Care Med. 2013;39:247–257.
5. Ari A and Fink JB: Inhalation therapy in patients receiving mechanical ventilation: An update. J Aerosol Med Pulm Drug Deliv. 2012;25:319–332.
6. Hess DR: Aerosol therapy during noninvasive ventilation or high-flow nasal cannula. Respir Care. 2015;60:880–893.
7. Dhand R: Inhalation therapy in invasive and noninvasive mechanical ventilation. Curr Opin Crit Care. 2007;13: 27–38.
8. Dhand R: Aerosol therapy in patients receiving noninvasive positive pressure ventilation. J Aerosol Med Pulm Drug Deliv. 2012;25:63–78.
9. Perry SA, Kesser KC, Geller DE, Selhorst DM, Rendle JK, and Hertzog JH: Influences of cannula size and flow rate on aerosol drug delivery through the vapotherm humidified high-flow nasal cannula system. Pediatr Crit Care Med. 2013;14:E250–E256.
10. Dugernier J, Hesse M, Jumetz T, Bialais E, Roeseler J, Depoortere V, Michotte J-B, Wittebole X, Ehrmann S, and Laterre P-F: Aerosol delivery with two nebulizers through high-flow nasal cannula: A randomized cross-over single-photon emission computed tomography study. J Aerosol Med Pulm Drug Deliv. 2017;30:349–358.
11. Reminiac F, Vecellio L, Heuze-Vourc'h N, Petitcollin A, Respaud R, Cabrera M, Le Pennec D, Diot P, and Ehrmann S: Aerosol therapy in adults receiving high flow nasal cannula oxygen therapy. J Aerosol Med Pulm Drug Deliv. 2016;29:134–141.
12. Longest PW, Walenga RL, Son Y-J, and Hindle M: High efficiency generation and delivery of aerosols through nasal cannula during noninvasive ventilation. J Aerosol Med Pulm Drug Deliv. 2013;26:266–279.
13. Longest PW, Spence BM, Holbrook LT, Mossi KM, Son Y-J, and Hindle M: Production of inhalable submicrometer aerosols from conventional mesh nebulizers for improved respiratory drug delivery. J Aerosol Sci. 2012;51:66–80.
14. Golshahi L, Tian G, Azimi M, Son Y-J, Walenga RL, Longest PW, and Hindle M: The use of condensational growth methods for efficient drug delivery to the lungs during noninvasive ventilation high flow therapy. Pharm Res. 2013;30:2917–2930.
15. Golshahi L, Longest PW, Azimi M, Syed A, and Hindle M: Intermittent aerosol delivery to the lungs during high flow nasal cannula therapy. Respir Care. 2014;59:1476–1486.
16. Golshahi L, Walenga RL, Longest PW, and Hindle M: Development of a transient flow aersol mixer-heater system for lung delivery of nasally administered aerosols using a nasal cannula. Aerosol Sci Technol. 2014;48:1009–1021.
17. Walenga RL, Longest PW, Kaviratna A, and Hindle M: Aerosol drug delivery during noninvasive positive pressure ventilation: Effects of intersubject variability and excipient enhanced growth. J Aerosol Med Pulm Drug Deliv. 2017; 30:190–205.
18. Dysart K, Miller TL, Wolfson MR, and Shaffer TH: Research in high flow therapy: Mechanisms of action. Respir Med. 2009;103:1400–1405.
19. Lenglet H, Sztrymf B, Leroy C, Brun P, Dreyfuss D, and Ricard J-D: Humidified high flow nasal oxygen during respiratory failure in the emergency department: Feasibility and efficacy. Respir Care. 2012;57:1873–1878.
20. Eschenbacher WL, Boushey HA, and Sheppard D: Alteration in osmolarity of inhaled aerosols cause bronchoconstriction and cough, but absence of a permeant anion causes cough alone. Am Rev Respir Dis. 1984;129:211–215.
21. Lowry RH, Wood AM, and Higenbottam TW: Effects of pH and osmolarity on aerosol-induced cough in normal volunteers. Clin Sci. 1988;74:373–376.
22. Walsh BK, Betit P, Fink JB, Pereira LM, and Arnold J: Characterization of ribavirin aerosol with small particle aerosol generator and vibrating mesh micropump aerosol technologies. Respir Care. 2016;61:577–585.
23. DiBlasi RM: Clinical controversies in aerosol therapy for infants and children. Respir Care. 2015;60:894–916.
24. Lindemann J, Leiacker R, Rettinger G, and Keck T: Nasal mucosal temperature during respiration. Clin Otolaryngol Allied Sci. 2002;27:135–139.
25. Anderson SD and Smith CM: Osmotic challenges in the assessment of bronchial hyperresponsiveness. Am Rev Respir Dis. 1991;991:543–546.
26. Hindle M and Longest PW: Condensational growth of combination drug-excipient submicrometer particles for targeted high efficiency pulmonary delivery: Evaluation of formulation and delivery device. J Pharm Pharmacol. 2012; 64:1254–1263.
27. Longest PW and Hindle M: Condensational growth of combination drug-excipient submicrometer particles: Comparison of CFD predictions with experimental results. Pharm Res. 2012;29:707–721.
28. Tian G, Hindle M, and Longest PW: Targeted lung delivery of nasally administered aerosols. Aerosol Sci Technol. 2014;48:434–449.
29. Tian G, Longest PW, Li X, and Hindle M: Targeting aerosol deposition to and within the lung airways using excipient enhanced growth. J Aerosol Med Pulm Drug Deliv. 2013;26:248–265.
30. Longest PW, Tian G, Li X, Son Y-J, and Hindle M: Performance of combination drug and hygroscopic excipient submicrometer particles from a softmist inhaler in a characteristic model of the airways. Ann Biomed Eng. 2012;40: 2596–2610.
31. Rubin BK and Williams RW: Emerging aerosol drug delivery strategies: From bench to clinic. Adv Drug Deliv Rev. 2014;75:141–148.
32. Longest PW and Hindle M: Quantitative analysis and design of a spray aerosol inhaler. Part 1: Effects of dilution air inlets and flow paths. J Aerosol Med Pulm Drug Deliv. 2009;22:271–283.
33. Hindle M and Longest PW: Quantitative analysis and design of a spray aerosol inhaler. Part 2: Improvements in mouthpiece performance. J Aerosol Med Pulm Drug Deliv. 2013;26:237–247.
34. ICRP: *Human Respiratory Tract Model for Radiological Protection*. Elsevier Science Ltd., New York; 1994.
35. Longest PW, Golshahi L, and Hindle M: Improving pharmaceutical aerosol delivery during noninvasive ventilation: Effects of streamlined components. Ann Biomed Eng. 2013;41:1217–1232.
36. Restrepo RD and Walsh BK: Humidification during invasive and noninvasive mechanical ventilation: 2012. Respir Care. 2012;57:782–788.
37. ASTM International: F1690-96 Standard Specification for Humidifiers for Medical Use. American Society for Testing Materials, West Conshohocken, PA; 2004.

38. Finlay WH: Estimating the type of hygroscopic behavior exhibited by aqueous droplets. J Aerosol Med. 1998;11: 221–229.
39. Longest PW and Hindle M: CFD simulations of enhanced condensational growth (ECG) applied to respiratory drug delivery with comparisons to in vitro data. J Aerosol Sci. 2010;41:805–820.
40. Longest PW and Xi J: Condensational growth may contribute to the enhanced deposition of cigarette smoke particles in the upper respiratory tract. Aerosol Sci Technol. 2008;42:579–602.
41. Wilcox DC: *Turbulence Modeling for CFD,* 2nd ed. DCW Industries, Inc., La Cañada Flintridge, CA; 1998.
42. Crowe C, Sommerfeld M, and Tsuji Y: *Multiphase Flows with Drops and Bubbles*. CRC Press, Boca Raton, 1998.
43. Longest PW and Hindle M: Numerical model to characterize the size increase of combination drug and hygroscopic excipient nanoparticle aerosols. Aerosol Sci Technol. 2011;45:884–899.
44. Longest PW, Tian G, Delvadia R, and Hindle M: Development of a stochastic individual path (SIP) model for predicting the deposition of pharmaceutical aerosols: Effects of turbulence, polydisperse aerosol size, and evaluation of multiple lung lobes. Aerosol Sci Technol. 2012;46: 1271–1285.
45. Longest PW, Hindle M, Das Choudhuri S, and Xi J: Comparison of ambient and spray aerosol deposition in a standard induction port and more realistic mouth-throat geometry. J Aerosol Sci. 2008;39:572–591.
46. Longest PW and Xi J: Effectiveness of direct Lagrangian tracking models for simulating nanoparticle deposition in the upper airways. Aerosol Sci Technol. 2007;41:380–397.
47. Vinchurkar S and Longest PW: Evaluation of hexahedral, prismatic and hybrid mesh styles for simulating respiratory aerosol dynamics. Comput Fluids. 2008;37:317–331.
48. Longest PW and Hindle M: Evaluation of the Respimat Soft Mist inhaler using a concurrent CFD and in vitro approach. J Aerosol Med Pulm Drug Deliv. 2009;22:99–112.
49. Longest PW, Azimi M, Golshahi L, and Hindle M: Improving aerosol drug delivery during invasive mechanical ventilation with redesigned components. Respir Care. 2014; 59:686–698.
50. Walenga RL, Tian G, Hindle M, Yelverton J, Dodson K, and Longest PW: Variability in nose-to-lung aerosol delivery. J Aerosol Sci. 2014;78:11–29.
51. Bennett G, Joyce M, Sweeney L, and MacLoughlin R: In vitro determination of the main effects in the design of high-flow nasal therapy systems with respect to aerosol performance. Pulm Ther. 2018;4:73–86.
52. Sunbul F, Fink JB, Harwood R, Sheard MM, Zimmerman RD, and Ari A: Comparison of HFNC, bubble CPAP and SiPAP on aerosol delivery in neonates: An in-vitro study. Pediatr Pulmonol. 2015;50:1099–1106.
53. Dailey PA, Harwood R, Walsh K, Fink JB, Thayer T, Gagnon G, and Ari A: Aerosol delivery through adult high flow nasal cannula with heliox and oxygen. Respir Care. 2018;62:1186–1192.
54. Zeman KL, Balcazar JR, Fuller F, Donn KH, Boucher RC, Bennett WD, and Donaldson SH: A trans-nasal aerosol delivery device for efficient pulmonary deposition. J Aerosol Med Pulm Drug Deliv. 2017;30:223–229.
55. Walenga RL, Longest PW, Kaviratna A, and Hindle M: Aerosol drug delivery during noninvasive positive pressure ventilation: Effects of intersubject variability and excipient enhanced growth. J Aerosol Med Pulm Drug Deliv. 2017; 30:190–205.
56. Hess DR: The mask of noninvasive ventilation: Principles of design and effects on aerosol delivery. J Aerosol Med. 2007;20:S85–S99.
57. Higgins R, Cookson W, Lane D, John S, McCarthy G, and McCarthy S: Cardiac arrhythmias caused by nebulised beta-agonist therapy. Lancet. 1987;330:863–864.
58. Küng M, Croley SW, and Phillips BA: Systemic cardiovascular and metabolic effects associated with the inhalation of an increased dose of albuterol: Influence of mouth rinsing and gargling. Chest. 1987;91:382–387.
59. Geller DE: Aerosol antibiotics in cystic fibrosis. Respir Care. 2009;54:658–670.
60. Corcoran TE, Godovchik JE, Donn KH, Busick DR, Goralski J, Locke LW, Markovetz MR, Myerburg MM, Muthukrishnan A, and Weber L: Overnight delivery of hypertonic saline by nasal cannula aerosol for cystic fibrosis. Pediatr Pulmonol. 2017;52:1142–1149.
61. Farkas D, Hindle M, and Longest PW: Efficient nose-to-lung aerosol delivery with an inline DPI requiring low actuation air volume. Pharm Res. 2018;35:194.
62. Daviskas E and Anderson SD: Hyperosmolar agents and clearance of mucus in the diseased airway. J Aerosol Med. 2006;19:100–109.

Received on July 27, 2018
in final form, January 4, 2019

Reviewed by:
Scott Donaldson
Laurent Vecellio
Jeffrey Schroeter

Address correspondence to:
*Worth Longest, PhD*
*Department of Mechanical and Nuclear Engineering*
*Virginia Commonwealth University*
*401 West Main Street*
*P.O. Box 843015*
*Richmond, VA 23284-3015*

*E-mail:* pwlongest@vcu.edu